

BAYESIAN INFERENCE APPLIED TO CRACK DETECTION IN BEAM-LIKE STRUCTURES

Héctor E. Goicoechea^{a,c}, Fernando S. Buezas^{a,d} and Marta B. Rosales^{b,c}

^a*IFISUR, Universidad Nacional del Sur, CONICET, Departamento de Física - UNS, Av. L. N. Alem
1253, B8000CPB - Bahía Blanca, Argentina*

^b*CONICET, Argentina, mrosales@criba.edu.ar*

^c*Departamento de Ingeniería, Universidad Nacional del Sur, Av. Alem 1253, (8000) Bahía Blanca,
Argentina*

^d*Departamento de Física, Universidad Nacional del Sur, Av. Alem 1253, (8000) Bahía Blanca,
Argentina*

Keywords: Crack detection, Cracked beam, Bayes, Bayesian Inference.

Abstract. In this work, a crack detection technique is presented by means of a bayesian inference approach. A simple non-linear model consisting of a slender beam subjected to transverse dynamic loads is considered. The nonlinearity is related to a breathing crack which is modelled as a bilinear spring. Given a certain crack configuration, the response of the system at specific locations is obtained (direct problem). These data are related to the crack configuration, depth and location. The aim of this work is the resolution of the inverse problem. That is, given a set of known responses (displacements) at specific points, the crack depth and location are sought i.e. level 3 of detection. For this purpose, the Bayesian Inference Method is used and the probability distributions of both the crack position and crack depth are obtained. As stated, this method is based on the Bayes Theorem which updates known statistical information (prior) giving place to a new statistics (posterior). This method was found to provide satisfying results, given limited available information.

1 INTRODUCTION

Cracks in a structural elements are not desirable and can indicate fatigue, mechanical problems or other defects in the manufacturing process (Rosales et al., 2009). Structural elements might be subjected to dynamic loading states under normal conditions, which is, for example, the case of a rotating shaft used in perforation processes in the oil industry. Therefore, identifying a cracked member before failure is of extreme importance to program the maintenance and to avoid excessive downtime in production processes.

Damage detection in a structure can be attained in four different levels (Rytter, 1993). **Level 1:** detection of the existence of damage; **Level 2:** Level 1 plus damage location; **Level 3:** Level 2 plus damage quantification; **Level 4:** Level 3 plus prediction of the remaining service life, usually uncoupled from the other three levels.

In the review by Doebling et al. (1998), Lifshitz and Rotem (1969) are mentioned as the first authors to publish the use of vibration data in damage identification. By that time, the computational resources and the experimental capacity to acquire and process data were very limited, which may explain why the first detection methods reported in literature are only based on natural frequency changes.

Back to the 1980s, with the introduction of finite elements as a powerful computational tool to model damaged structural elements, the frequency change criterion became the most studied (Salawu, 1997; Dimarogonas, 1996; Owolabi et al., 2003; Kim and Stubbs, 2003), and the detection of many different crack configurations with this technique was reported in Dimarogonas (1996); Owolabi et al. (2003); Kim and Stubbs (2003); Khiem and Lien (2004).

Some attempts to detect damage from the resolution of the inverse problem were included in studies performed by Law and Lu (2005) and by Rao and Rahman (2006), but the bad conditioning of the problem makes damage detection difficult to be tackled as a pure inverse problem. Many works dealing with straight beams have been reported (Doebling et al., 1998).

On the other hand, Wang and He (2007) used artificial neural networks (ANN) to detect crack in arch structural elements, while the authors of the present work have employed ANN in beam-like structures and rotating beams (Rosales et al., 2009).

Many of the methods to detect cracks in beam-like structures are based on linear one-dimensional models and are not straightforwardly applicable to structures such as beams or arcs with an open crack or a breathing crack with or without contact. For such cases, genetic algorithms appear as an attractive approach (Houck and Kay, 2008; Buezas et al., 2008) to optimize an objective function that depends on the crack position and magnitude when nonlinear dynamics are present, and large rotations or contact at the closing crack occur. Research in this direction can be found in Carneiro and Inman (2002, 2001); Carlin and Garcia (1996); Raous (1999).

Finally, contact at the crack can be modelled in many ways. Carneiro (2000) proposed a breathing crack model for a Timoshenko beam, while the present authors present a pure non-linear Theory of Elasticity like approach.

The present study deals with one-dimensional models to handle the dynamics of a structural element with a transverse breathing crack. The methodology is not only restricted to beam-like structures but it can be also applied to any arbitrary shaped 3D element. The crack is simulated as a notch with a unilateral contact model (non linear part of the problem) calculated with a 3-D elasticity theory model, in order to get an equivalent rotational spring coefficient. Then, this coefficient is used as an external parameter in the Bernoulli-Euler equation. All the simulations are carried out using the finite element code FlexPDE (PDE-Solutions, 2016), a general purpose

partial differential equation solver.

A robust optimisation method based on Bayes formula is successfully employed for crack detection. The dynamic response at some points of the damaged structure is collected and then a probability density function is constructed.

The optimisation algorithm is developed within the MATLAB (MathWorks, 2016) environment and interacts with the FEM model. Extensive studies were carried out to analyse the influence of the various parameters involved in the bayesian algorithm.

2 PHYSICAL MODEL

A simple problem consisting of a slender cracked beam subjected to an initial velocity field is analysed. The crack is modelled as a breathing crack. It opens and closes depending on the curvature of the beam. The structural element can be thought as consisting of two healthy beams connected via a rotational spring, which simulates the effects of the crack. The geometry of the problem is shown in Figure 1, and described in Table 1.

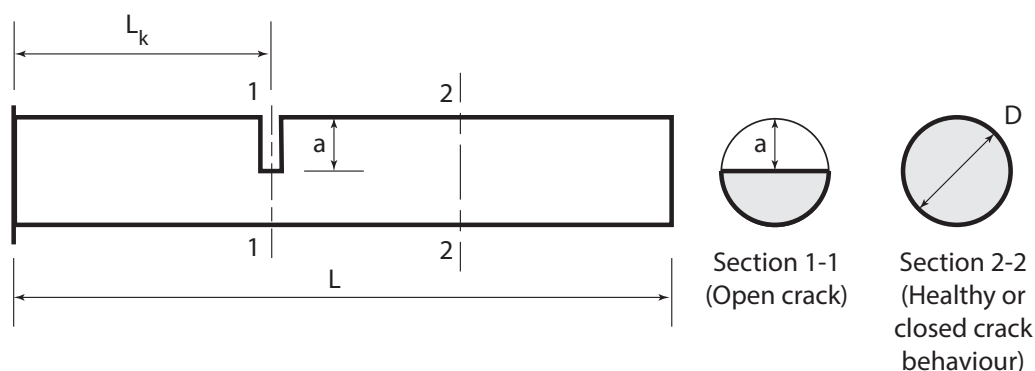


Figure 1: Geometry of the analysed beam in both healthy and cracked cross-sections.

Property	Symbol	Value
E	Elastic modulus	2.1 MPa
ρ	Density	7800 kg/m ³
D	Diametre	1 m
L	Length	10 m

Table 1: Material and geometric properties.

In this approach, a crack configuration is defined by its depth a and position L_k . This crack geometry is normal to the axis of the beam and extends within its depth to the full width of the cross-section. The beam is divided into three regions: two healthy sides and a linking short beam of reduced section that will be modelled by an equivalent spring (Dimarogonas and Papadopoulos, 1983).

In order to reduce the real model to a simpler 1-D Euler model, the effects of the equivalent spring and the cracked section in the real structure need to be the same, meaning that both deformations and internal efforts should coincide. For this task, Euler theory cannot be used in the determination of the spring constant as the slenderness hypothesis is not true.

One way to obtain the equivalent spring coefficient is to perform a study of the local flexibility of the beam by means of fracture mechanics (Dimarogonas and Papadopoulos, 1983). Another possibility is adopted in this work: an associated rotational spring coefficient is obtained by application of Elasticity theory on a 3-D model. A loading state consisting of a force P applied at the right end of the beam is considered.

Displacements obtained from the 3-D model should be consistent and equal to displacements evaluated with the 1-D Euler model proposed in Figure 2

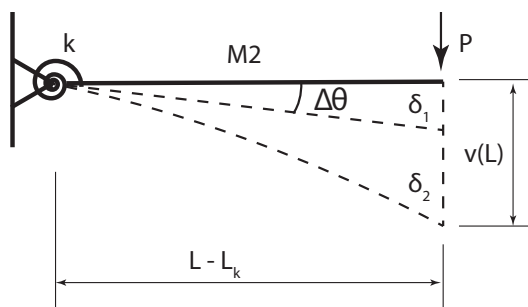


Figure 2: 1-D model employed in the evaluation of the equivalent spring.

In the 1-D model, the displacement at the tip of the beam $v(L)$ can be expressed as a combination of the displacements δ_1 due to a rigid rotation provoked by the loss of rigidity at the crack, and δ_2 due to the deformation of the healthy side of the beam. Therefore, the rigid rotation can be expressed as:

$$\Delta\theta = \frac{v(L) - v_0(L)}{L - L_k} \quad (1)$$

where $v(L)$ is the deformation at the tip of the beam for any crack configuration and $v_0(L)$ the deformation for an uncracked beam. Then, the equivalent spring coefficient can be written as:

$$k = \frac{M}{\Delta\theta} = \frac{M \cdot (L - L_k)}{\Delta\theta} = \frac{P \cdot (L - L_k)^2}{v(L) - v_0(L)} \quad (2)$$

In order to numerically quantify k for different crack configurations, displacements $v(L)$ and $v_0(L)$ obtained from the 3-D model are introduced into Equation 2. Different values for the equivalent spring stiffness coefficient k have been numerically obtained for various relative crack lengths a/D , and are shown in Figure 3. Software FlexPDE has been used in the resolution of the differential equations.

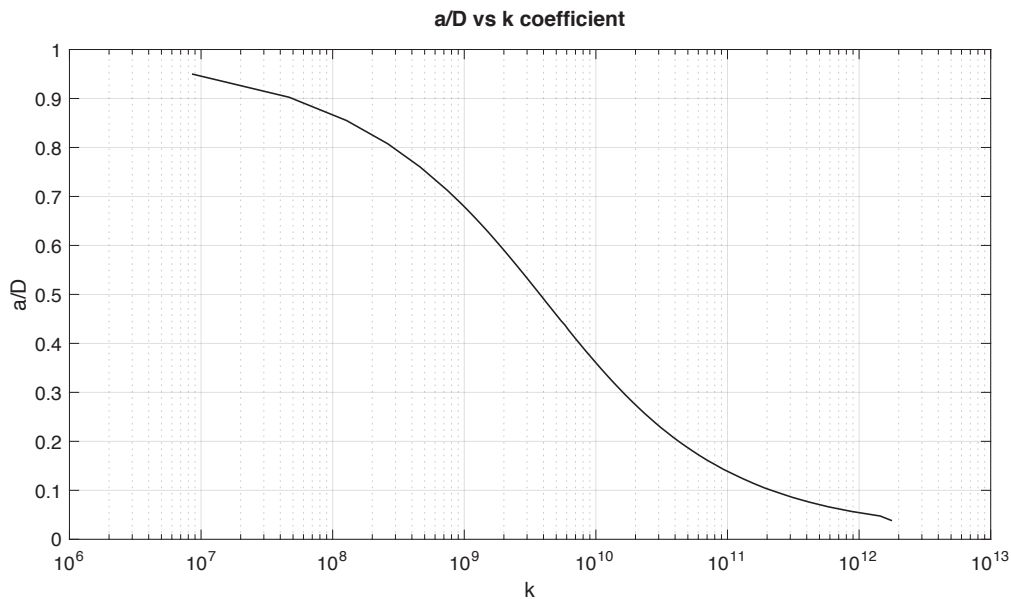


Figure 3: Relative crack depth (a/D) vs equivalent spring coefficient (k).

Finally, the associated 1-D model for the cracked beam is presented in Figure 4, where $M1$ and $M2$ represent the two healthy parts of the beam, and k represents the equivalent rotational spring.

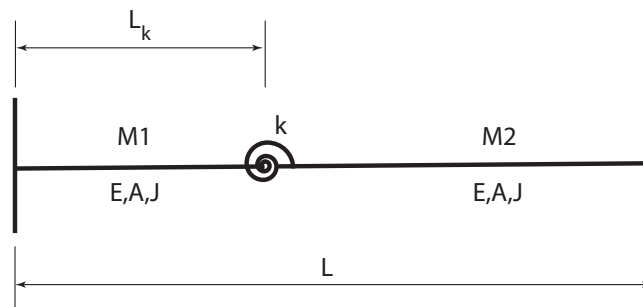


Figure 4: Representation of the 1-D cracked beam model.

2.1 Inverse Problem

The objective of this work is to obtain a solution for the inverse problem using the Bayes Theorem. To this purpose, a cracked beam under the influence of an external action is analysed and some measurable data are collected. Then, the probability density functions (PDFs) associated to the dynamics are constructed and the inverse problem is solved by means of the application the Bayes Theorem, which derives from the definition of conditional probability.

If Θ represents a set of unknown parameters to be determined indirectly, and D represents measurable data, the Bayes Theorem enables the obtainment of the sought PDF (output), usually referred to as posterior PDF, by combining known information (prior PDF) and experimental values of the observed response (likelihood PDF).

The idea of the method is simple and the main challenge lies in finding an expression for the likelihood PDF. As previously stated, the information required for its construction is related to measurable data from an experiment. In this work, displacement values are used.

The prior PDF is related to previous knowledge about the parameters. If no prior information is available then every value has the same occurrence probability, thus a uniform PDF is appropriate.

The Bayes Theorem is mathematically stated as follows:

$$\rho_{post}(\Theta | D) = \frac{\rho_{pr}(\Theta) \cdot \rho_l(D | \Theta)}{P(D)} \quad (3)$$

where Θ stands for the parameters and D for the associated data. The sought PDF, noted as $\rho_{post}(\Theta | D)$, is the posterior PDF, $\rho_{pr}(\Theta)$ is the prior PDF, $\rho_l(D | \Theta)$ is the likelihood PDF, and $P(D)$ is a normalisation factor. In this example $\Theta = (L_k, a)$, where L_k and a are independent variables.

The solution of this equation can be numerically obtained by the application of a Metropolis-Hastings MCMC method, with the advantage that there is no need to numerically quantify the value of $P(D) = \int \rho_{pr}(\Theta) \cdot \rho_l(D | \Theta) \cdot d\theta$, in general a multidimensional integral, since the algorithm relies on a ratio in which this quantity vanishes.

2.2 Experimental Data

The application of the Bayes Theorem requires the construction of a likelihood PDF based on collected data from the response of the structure, for which an experiment has to be performed. The experiment consists in the observation of the response of the structure to an external action such as an initial displacement, an initial velocity field, fluctuating forces, impact forces, etc.

In this work, we will obtain the likelihood PDF by numerically simulating the experiment. We will call this simulation a "synthetic experiment" and L_{si} the position of a "sensor", that is the position of the point where data will be collected.

The procedure consists on performing a stochastic analysis due to uncertainties on the properties of the crack. To perform this task, first the direct problem needs to be solved. A distribution for each independent parameter is proposed. The depth of the crack, namely $a \in [0, D]$, is supposed to have a truncated gaussian distribution centred at $\mu_c = 0.5m$ with a standard deviation $\sigma_c = 0.05$. The position of the crack $L_k \in [0, D]$ follows a proposed truncated gaussian distribution centred at $\mu_k = 8m$ with a standard deviation $\sigma_k = 0.20$.

The beam starts the motion after an initial condition given by a velocity field. Then, the direct problem is solved a large number of times for different crack configurations and the output is used to generate the sought PDF based on displacement data.

2.3 Application of Bayes Theorem

In order to obtain an acceptable reliability using the smallest amount of information, a convergence analysis will be carried out. To this purpose, two different set of experiments, named A and B, will be performed.

In the "A" set of experiments, maximum and minimum displacements found for time $t = [0; 0.3s]$ with sensors located at L_{si} are used to generate the likelihood PDF; while in the "B" set of experiments, displacements are evaluated at $t = [0(0.02)0.3s]$ with sensors located at L_{si} . Table 2 shows sensor configuration for each experiment.

When generating the likelihood PDF, each different combination of sensor position and time

Experiment	Number of Sensors	Sensor Position $L_{si}[m]$
A1	1	{10}
A2	2	{5; 10}
A3	4	{2.5; 5; 7.5; 10}
A4	8	{1.25; 2.5; 3.75; 5; 6.25; 7.5; 8.75; 10}
B1	1	{10}
B2	2	{5; 10}
B3	4	{2.5; 5; 7.5; 10}

Table 2: Description of sensor configuration for each experiment performed.

(L_{si}, t_i) constitutes a different variable, thus a multidimensional likelihood PDF is constructed by means of a kernel smoothing method (Bowman and Azzalini, 1997).

Next, the Bayes Theorem is applied and samples from the posterior PDF are taken using a Metropolis-Hastings MCMC algorithm. Since the method is based on a Markov chain, it relies on evaluating the acceptance ratio of the current proposed sample in relation to the previous accepted sample, therefore, the way in which a new possible sample is proposed needs to be defined.

The distribution employed to propose a new sample is called the proposal PDF. Given that both L_k and a are independent variables, this distribution can be written in terms of the products: $\rho_{prop}(\Theta) = \rho_{prop}(L_k) \cdot \rho_{prop}(a)$. The parameters that define each chosen proposal PDF are presented in Table 3.

PDF	Distribution Type	Support	Deviation σ
$\rho_{prop}(L_k)$	Truncated Normal Distribution	$[0, L_k]$	0.8
$\rho_{prop}(a)$	Truncated Normal Distribution	$[0, a]$	0.1

Table 3: Chosen proposal distributions for the Metropolis-Hastings method.

Finally, the found Θ values are used to construct the posterior PDF $\rho(\Theta|D)$. As previously stated, since the parameters $\Theta = (L_k, a)$ are independent, it is assumed that $\rho_{post}(\Theta|D) = \rho(L_k|D) \cdot \rho(a|D)$. Consequently, a one dimension PDF for each sought parameter can be reconstructed, once again, by means of a kernel smoothing method.

For each experiment performed, 15000 samples have been obtained, from which 500 samples have considered part of a burn-in period.

3 RESULTS

A synthetic experiment was used to collect the information required for the application of the theorem. The likelihood PDF was created by proposing a distribution for L_k and a . Thus, the solution of the inverse problem, if it were exact, should match the proposed distributions for the parameters. Letter E will be used to denote the target solution.

3.1 Series A of experiments

In this section, the results corresponding to the series A of experiments are presented. An evaluation of the convergence for both L_k and a is performed. Let us remind that the maximum and minimum displacements from the temporal response were used, as indicated in Table 2.

Figure 5 depicts the obtained posterior PDF $\rho(L_k|D)$; Figure 6, the evolution of the associated mean and deviation value for L_k ; Figure 7, the obtained posterior PDF $\rho(a|D)$; and Figure

8, the associated mean and deviation values for a .

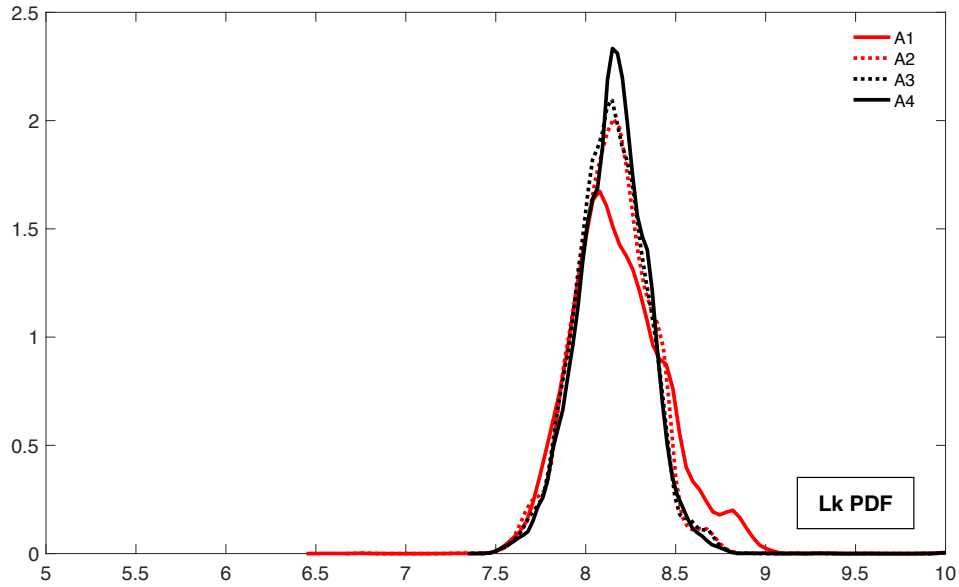


Figure 5: Graphical representation of the Posterior PDFs $\rho(L_k|D)$ for the series A of experiments.

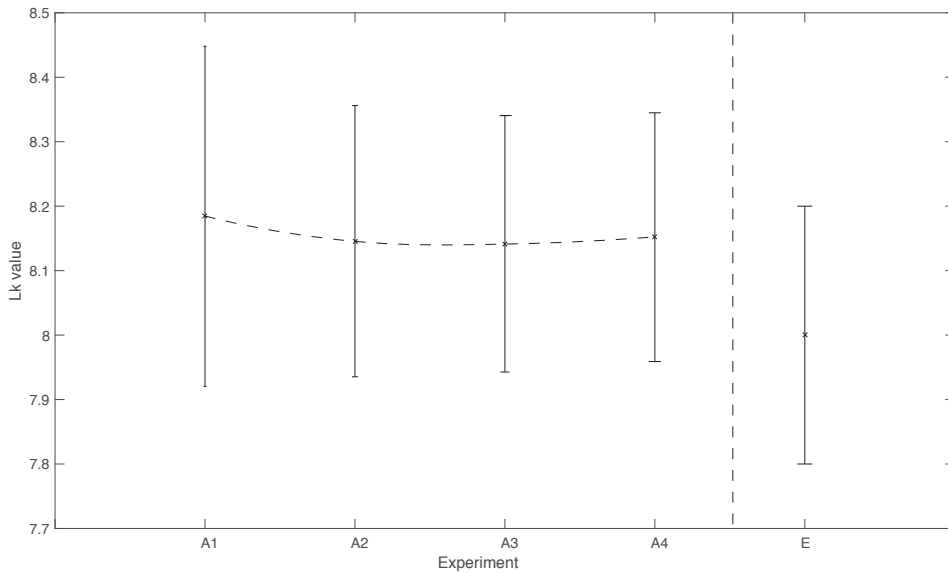


Figure 6: Graphical representation of the mean and deviation value of the Posterior PDFs $\rho(L_k|D)$ for the series A of experiments. Case E denotes the expected exact solution.

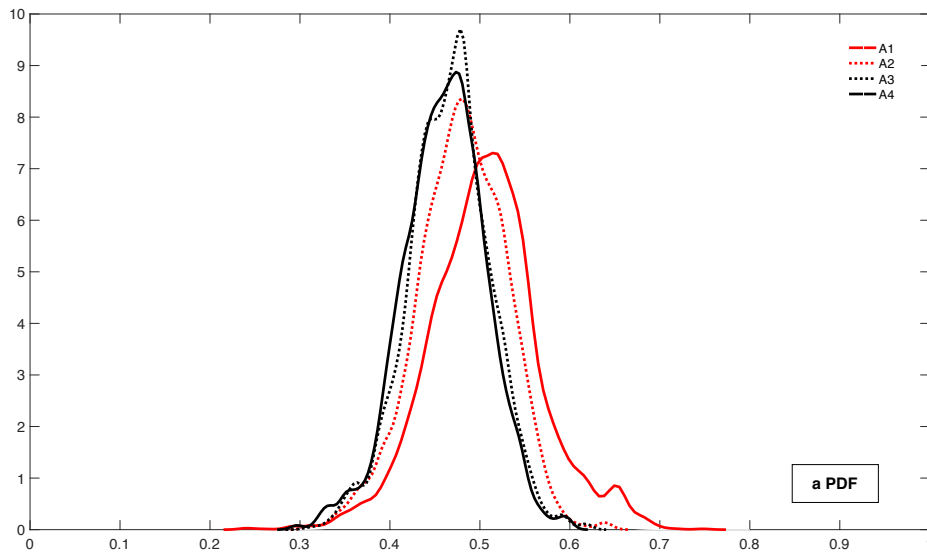


Figure 7: Graphical representation of the Posterior PDFs $\rho(a|D)$ for the series A of experiments.

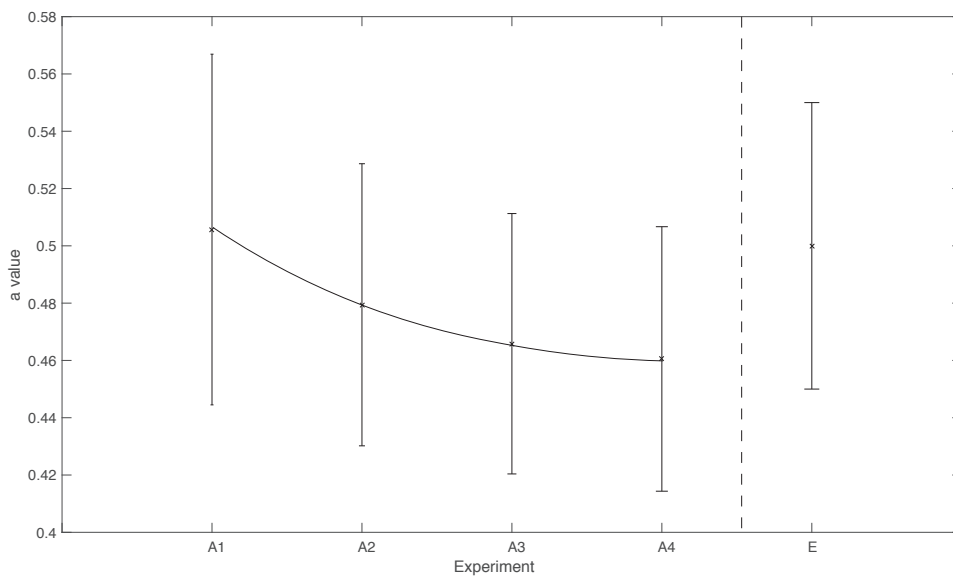


Figure 8: Graphical representation of the mean and deviation value of the Posterior PDFs $\rho(a|D)$ for the series A of experiments. Case E denotes the expected exact solution.

Experiment A1 exhibits the highest deviation value, as shown in Figures 6 and 8, while for the rest of the series, the deviation seems to remain at a constant value.

In relation to the mean of the sought parameters, for L_k a rather constant value is found for

all experiments; while for a , the mean seems to converge to a value lower than the expected one.

A direct observation of the results suggests that increasing to two sensors improves the accuracy, while the use of more than two sensors does not seem to dramatically improve results.

3.2 Series B of experiments

In this section, the results corresponding to the series B of experiments are presented. An evaluation of the convergence for both L_k and a is performed. As mentioned before, this series of experiments employs a larger amount of values from the temporal response. The results are compared with the series A of experiments to analyse if there is any improvement in the accuracy.

Figure 9 depicts the obtained posterior PDF $\rho(L_k|D)$; Figure 10, the evolution of the associated mean and deviation value for L_k ; Figure 11, the posterior PDF $\rho(a|D)$; and Figure 12, the associated mean and deviation values for a .

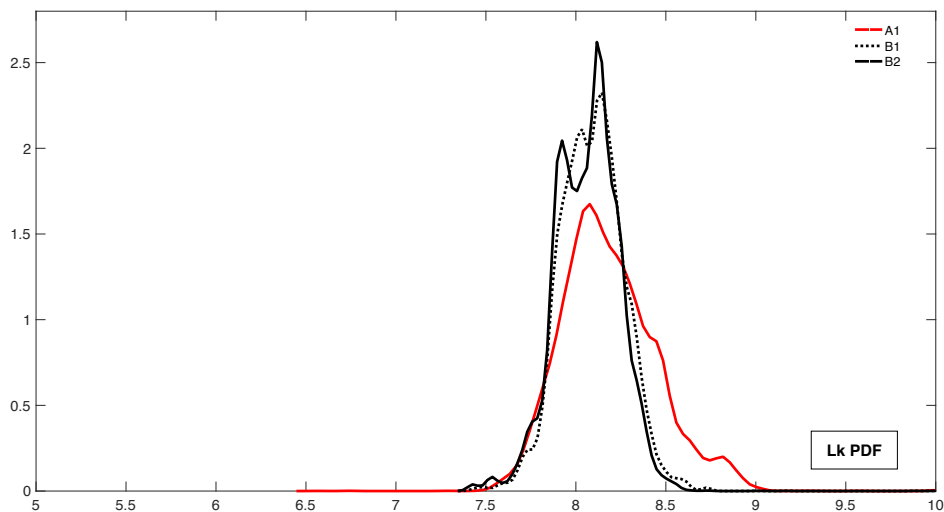


Figure 9: Graphical representation of the Posterior PDFs $\rho(L_k|D)$ for the series B of experiments.

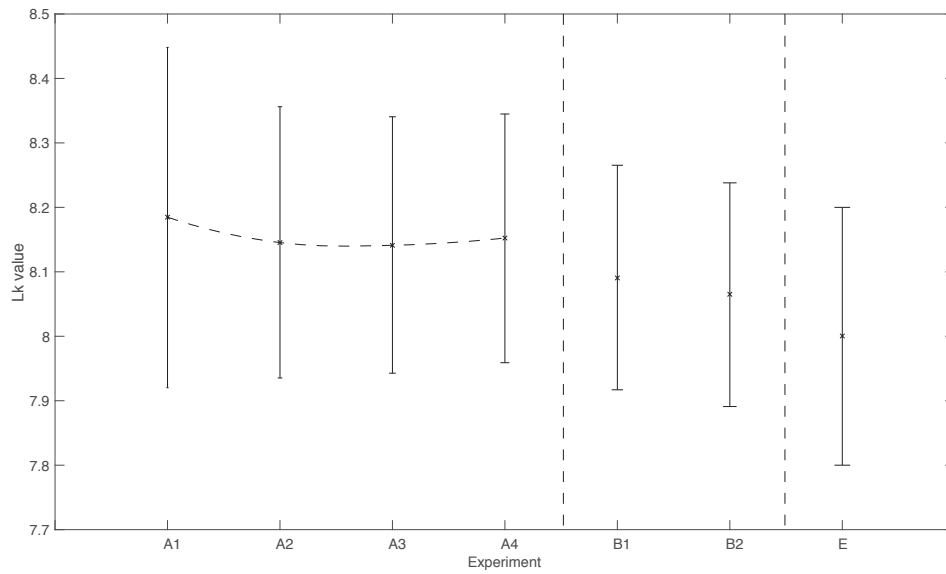


Figure 10: Graphical representation of the mean and deviation value of the Posterior PDFs $\rho(L_k|D)$ for the series A and B of experiments. Case E denotes the expected exact solution.

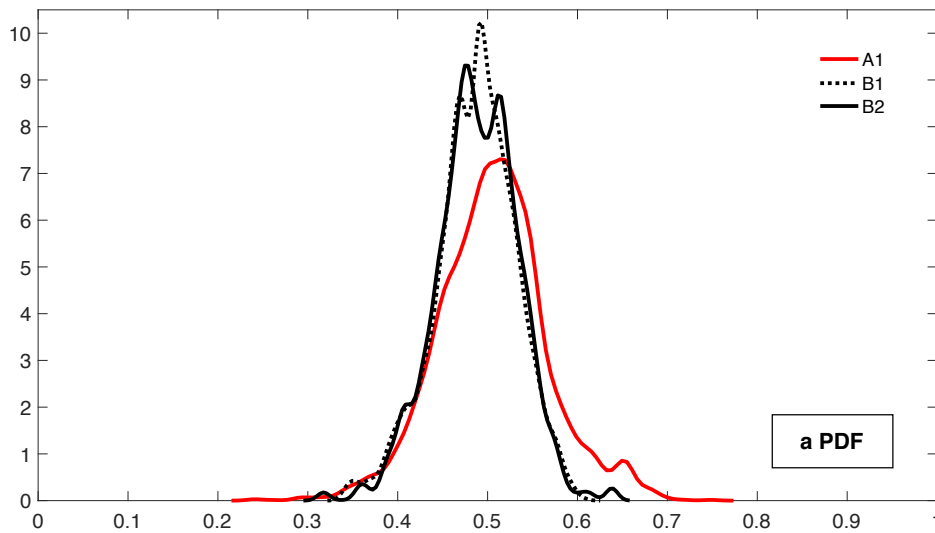


Figure 11: Graphical representation of the Posterior PDFs $\rho(a|D)$ for the B series of experiments.

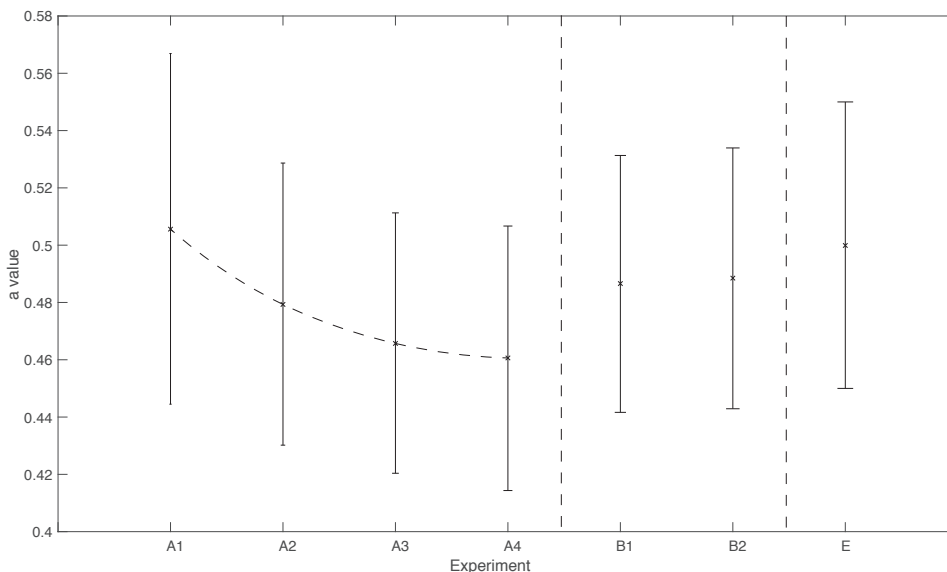


Figure 12: Graphical representation of the mean and deviation value of the Posterior PDFs $\rho(a|D)$ for the series A and B of experiments. Case E denotes the expected exact solution.

A summary of the observed mean and deviation values is presented in Table 4. Figure 10 and Figure 12 show a more accurate mean value for both L_k and a and their associated deviations, if compared to the A series. This is an expected result, as more information from the temporal response has been used.

For the series B, the addition of more than one sensor does not dramatically increase the accuracy.

Experiment	μ_a	σ_a	$CV(a)$	μ_{L_k}	σ_{L_k}	$CV(L_k)$
A1	0.5057	0.0612	0.1210	8.1841	0.2640	0.0323
A2	0.4749	0.0492	0.1036	8.1457	0.2104	0.0258
A3	0.4658	0.0454	0.0975	8.1516	0.1989	0.0244
A4	0.4605	0.0462	0.1003	8.1519	0.1929	0.0237
B1	0.4865	0.0448	0.0921	8.0912	0.1742	0.0215
B2	0.4884	0.0455	0.0932	8.0645	0.1735	0.0215
E	0.5000	0.0500	0.1000	8.0000	0.2000	0.0250

Table 4: Mean, standard deviation and coefficient of variation the parameters L_k and a for each experiment performed. Case E denotes target values.

4 CONCLUSIONS

The main objective of this work is the resolution of the inverse problem using a Bayesian algorithm for crack detection. This is done from limited kinematic information collected in an experiment. A robust optimization is performed and probability distributions of the sought parameters are found.

The methodology constitutes a useful tool for the resolution of the inverse problem, and

particularly in cracked structures, with a stochastic approach, based on indirect and sparse information.

The series B of experiments exhibits, for any amount of physical sensors, higher accuracy than series A. Employing more information from the temporal response improves accuracy and is preferred over an increase in the amount of sensors.

The method has been successful in solving the inverse problem. A comparison between a bayesian approach and other methods, such as artificial neural networks (ANNs) would be interesting to evaluate the performance and the convenience of the application of different methodologies.

REFERENCES

- Bowman A.W. and Azzalini A. *Applied Smoothing Techniques for Data Analysis*. 1997. ISBN 0191545694.
- Buezas F.S., Rosales M.B., and Filipich C.P. Damage Detection in Structural Elements Taking Into. *Mecánica Computacional*, XXVII:10–13, 2008.
- Carlin R. and Garcia E. Parameter optimization of a genetic algorithm for structural damage detection. *Proceedings of the 14th International Modal Analysis Conference (IMAC)*, pages 1292–1298, 1996.
- Carneiro S.H.S. *Model-based vibration diagnostic of cracked beams in the time domain*. Ph.D. thesis, Faculty of the Virginia Polytechnic Institute and State University, 2000.
- Carneiro S.H.S. and Inman D.J. Comments on the Free Vibrations of Beams With. 244:729–736, 2001.
- Carneiro S.H.S. and Inman D.J. Continuous Model for the Transverse Vibration of Cracked Timoshenko Beams. *Journal of Vibration and Acoustics*, 124(2):310–320, 2002.
- Dimarogonas A.D. Vibration of cracked structures: A state of the art review. *Engineering Fracture Mechanics*, 55(5):831–857, 1996.
- Dimarogonas A.D. and Papadopoulos C.A. Vibration of cracked shafts in bending. *Journal of Sound and Vibration*, 91(4):583–593, 1983.
- Doebbling S.W., Farrar C.R., and Prime M.B. A Summary Review of Vibration-Based Damage Identification Methods. *Shock & Vibration Digest*, 30(2):91, 1998.
- Houck C.R. and Kay M.G. A Genetic Algorithm for Function Optimization : A Matlab Implementation. *Ncsuie Tr*, 95(919):1–14, 2008.
- Khiem N. and Lien T. Multi-crack detection for beam by the natural frequencies. *Journal of Sound and Vibration*, 273(1-2):175–184, 2004.
- Kim J.T. and Stubbs N. Crack Detection in Beam-Type Structures Using Frequency Data. *Journal of Sound and Vibration*, 259(1):145–160, 2003.
- Law S.S. and Lu Z.R. Crack identification in beam from dynamic responses. *Journal of Sound and Vibration*, 285(4-5):967–987, 2005.
- MathWorks. MATLAB. 2016.
- Owolabi G.M., Swamidas A.S.J., and Seshadri R. Crack detection in beams using changes in frequencies and amplitudes of frequency response functions. *Journal of Sound and Vibration*, 265(1):1–22, 2003.
- PDE-Solutions. FlexPDE 6.39. 2016.
- Rao B.N. and Rahman S. A continuum shape sensitivity method for fracture analysis of isotropic functionally graded materials. *Computational Mechanics*, 38(2):133–150, 2006.
- Raous M. Quasistatic Signorini Problem with Coulomb Friction and Coupling to Adhesion. In *New Developments in Contact Problems*, volume 384, chapter 3, pages 101–178. 1999.

- Rosales M.B., Filipich C.P., and Buezas F.S. Crack detection in beam-like structures. *Engineering Structures*, 31(10):2257–2264, 2009.
- Rytter A. *Vibrational Based Inspection of Civil Engineering Structures*. Ph.D. thesis, Aalborg University, 1993.
- Salawu O. Detection of structural damage through changes in frequency: a review. *Engineering Structures*, 19(9):718–723, 1997.
- Wang B. and He Z. Crack detection of arch dam using statistical neural network based on the reductions of natural frequencies. *Journal of Sound and Vibration*, 302(4-5):1037–1047, 2007.